Vol 16 No 7, July 2007
1009-1963/2007/16(07)/2123-08

Chinese Physics

© 2007 Chin. Phys. Soc.
and IOP Publishing Ltd

Theoretical investigation of exchange bias*

Xiong Zhi-Jie(熊知杰)[a], Wang Huai-Yu(王怀玉)[b]†, and Ding Ze-Jun(丁泽军)[a]

[a] *Department of Physics, University of Science and Technology of China, Hefei* 230026, *China*
[b] *Department of Physics, Tsinghua University, Beijing* 100084, *China*

(Received 24 November 2006; revised manuscript received 18 January 2007)

The exchange bias of bilayer magnetic films consisting of ferromagnetic (FM) and antiferromagnetic (AFM) layers in an uncompensated case is studied by use of the many-body Green's function method of quantum statistical theory. The effects of the layer thickness and temperature and the interfacial coupling strength on the exchange bias $H_{\rm E}$ are investigated. The dependence of the exchange bias $H_{\rm E}$ on the FM layer thickness and temperature is qualitatively in agreement with experimental results. When temperature varies, both the coercivity $H_{\rm C}$ and $H_{\rm E}$ decrease with the temperature increasing. For each FM thickness, there exists a least AFM thickness in which the exchange bias occurs, which is called pinning thickness.

Keywords: exchange bias, coercivity, uncompensated case, Heisenberg Hamiltonian
PACC: 7510J, 7570F, 7570A

1. Introduction

Exchange bias (EB) is a shift of a hysteresis loop due to a unidirectional anisotropy. This anisotropy is caused by the exchange coupling at the interface between ferromagnetic (FM) and antiferromagnetic (AFM) materials after the sample has been cooled in a magnetic field through the Néel temperature of the AFM.[1,2] The phenomenon of EB was observed in many different systems containing FM–AFM interfaces, such as magnetic oxides,[1] inhomogeneous bulk materials[3] and thin films.[4−6] Possible applications of EB include permanent magnets, magnetic recording media or domain stabilizers in recording heads. The application prospect of EB has aroused both experimental and theoretical interest for decades. In this paper, we will study the EB of the FM/AFM bilayers, because they are believed to be more amenable to the development of devices than other FM/AFM systems.

To explain the EB effect, theoretical models such as the phenomenal model,[1] random-field model,[7] micromagnetic theory,[8] spin-wave theory,[9] domain state model,[10] etc, have been suggested. Kiwi[11] reviewed the relevant theoretical work. Each model may explain one or more aspects of EB, but cannot be well supported by experiments in other aspects.[11] These theoretical results are often two or three orders of magnitude larger than those observed in most of the FM/AFM systems. Studies on the EB in FM/AFM bilayers have therefore been developed in two trends, as pointed by Thuy *et al.*[12] One is to bring the experimental values of $H_{\rm E}$ closer to those predicted by theories. This has been realized by improving the preparation techniques and looking for novel materials having larger unidirectional anisotropy. The other is to develop theoretical computation to give numerical results closer to the experimentally obtained EB values. In this paper, we evaluate the EB values one order of magnitude larger than experimental ones, which is thought as an improvement in theoretical work. We confess that the model used in this paper is ideal, and the technical magnetism cannot be considered. The question of how to consider the technical magnetism theoretically in studying EB is still open.

The model to be suggested is guided by the following two considerations. On the one hand, for qualitative description, the model should be as simple as possible. As pointed out by Kiwi,[11] the insight derived from the understanding of simple systems can well prove to be transferable to more complex cases. On the other hand, we believe that a quantum-mechanical model should be an appropriate means to explore the microscopic origin of EB. In this paper, we show that a simplest Heisenberg model can reveal physical characteristics of EB. In our model we use only the fact that

*Project supported by the National Natural Science Foundation of China (Grant Nos 10574121, 90406024 and 10025420), Chinese Education Ministry and Chinese Academy of Sciences.
†E-mail: wanghuaiyu@mail.tsinghua.edu.cn

an FM layer is deposited by an AFM layer without need to resort to the technical magnetism of the materials, spin flop[13] and the spiral spin structures.[14] Quantum statistical theory is used to calculate the coercivity $H_{\rm C}$ and the loop shift $H_{\rm E}$ as functions of layer thickness, temperature and the coupling strength across the FM/AFM interface.

There are two kinds of cases in considering the spin arrangement of AFM films. One is called uncompensated case (UCC), in which there is a net magnetization in the AFM surface. The other is called compensated case (CC), in which there is no net magnetization in the AFM surface. In this paper, we restrict ourselves to the case of UCC.

Exchange bias is essentially an interfacial effect.[2] For UCC, the intuitive picture of exchange bias is clear. In Ref.[15], based on the experimental results in Ref.[16], Wang *et al* suggested a frozen model that simplified the AFM layer into a magnetic moment of a single monolayer (ML). The spins of this ML were frozen in a wide temperature range under its Néel point and did not vary with the magnetic field. The effect of this net magnetization was to apply an exchange bias field (EBF) to the FM layer. Unfortunately, this model was too simple. Actually, the net magnetization of AFM surface at the interface should depend on the temperature and external field. In this paper, we consider that the AFM layer has a finite thickness, so that the model is closer to the practical physical systems. Because there exists a net magnetization at the AFM surface, the conception of the EBF can still be applied as was done in Ref.[15]. Obviously, the EBF is dependent on the temperature, external field, and thickness of AFM layer, unlike the case of Ref.[15] where it was fixed.

In the following, we introduce the model Hamiltonian and the method used in Section 2, and then numerically calculate the magnetization of the FM/AFM film under the variation of the temperature and the film thickness in the absence of external field in Section 3. We think that it is helpful for our discussion to define a total magnetization and an averaged magnetization. The main part of this paper is for the investigation of the exchange bias. Exchange bias $H_{\rm E}$ and coercivity $H_{\rm C}$ are calculated, and the effects of temperature, layer thickness, interfacial exchange strength are also investigated. The last section, i.e. Section 4, is for our summary.

2. Hamiltonian and method

The model studied is depicted in Fig.1. It is consistent with the physical picture in Nogues and Schuller's review article.[2] The system contains L MLs. The thicknesses of the FM and AFM layers are L_1 and L_2 MLs, respectively. $L_1 + L_2 = L$. The crystal structure is assumed to be a simple cubic lattice. The normal of the film is [100]. The Hamiltonian is

$$H = -\sum_{\alpha=1}^{L} J_\alpha \sum_{(i,j)} S_{\alpha i} S_{\alpha j} - \sum_{\alpha=1}^{L-1} \sum_{i} J_{\alpha\alpha-1} S_{\alpha i} S_{\alpha+1 j} - \sum_{\alpha=1}^{L} K_\alpha \sum_{i} (S_{\alpha i}^z)^2 - \sum_{i} B S_{\alpha i}^z. \quad (1)$$

On the right-hand side of the above expression, the first term is the Heisenberg exchange energy in each ML. Greek letter α labels MLs, and i and j denote the spin sites in each monolayer. J_α is the FM exchange parameter in each ML. Here only the neighbouring exchange is considered. The second term is Heisenberg exchange energy between neighbouring MLs. The L_1th ML and the (L_1+1)th ML are interfaces. The couplings between neighbouring MLs in FM layer are ferromagnetic and those in AFM layer are antiferromagnetic. The third term describes the single-ion anisotropic energy which shows that the z-axis is the easy axis. The strength of K is usually believed to be two orders of magnitude less than J.[17,18] The last term is the Zeeman energy when an external field is applied along the z-direction.

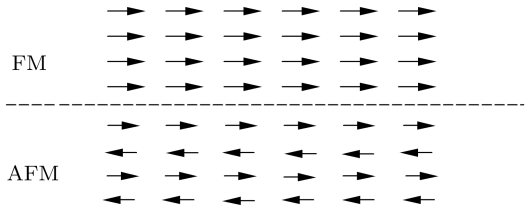


Fig.1. UCC model of the FM/AFM bilayer.

The many-body Green's function method (MBGFM) of quantum statistical theory is used to calculate the magnetization. This method is valid in the whole temperature range and takes into account the spin fluctuation. The retarded Green's function is defined as[19]

$$G_{ij}(t-t') = \langle\langle A_i; B_j \rangle\rangle = -\mathrm{i}\theta(t-t')\langle A_i B_j - B_j A_i \rangle, \quad (2)$$

where $\langle A\rangle$ represents the statistical average of the physical quantity A in a canonical ensemble. The Green's function is time Fourier transformed and then we obtain the equation of motion

$$\omega\langle\langle A_i; B_j\rangle\rangle = \frac{1}{2\pi}\langle[A_i, B_j]\rangle + \langle\langle[A_i, H]; B_j\rangle\rangle. \quad (3)$$

Now we choose $A_i = S_i^+$. The following derivation process is somewhat similar to that in Ref.[20]. The higher-order Green's functions are decoupled by random phase approximation as follows:

$$\langle\langle S_l^z S_i^+; B_j\rangle\rangle = \langle S_l^z\rangle\langle\langle S_i^+; B_j\rangle\rangle, \quad l \neq i. \quad (4)$$

As for the higher-order Green's function concerning single-ion anisotropy, we adopt the Anderson and Callen's decomposition,[21] instead of the Lines' decoupling[22] as used in Ref.[20],

$$\langle\langle S_i^z S_i^+ + S_i^+ S_i^z; B_j\rangle\rangle = 2C_1\langle S_i^z\rangle\langle\langle S_i^+; B_j\rangle\rangle, \quad (5)$$

where

$$C_1 = 1 - \frac{1}{2S^2}[S(S+1) - \langle(S^z)^2\rangle]. \quad (6)$$

This is a widely applied decomposition form,[23,24] and it is applicable to any spin quantum number. The Monte Carlo calculation[25] showed that this decoupling way was a comparatively good approximation when K was not large.

By using the commutator of S_i^+ and the Hamiltonian, and the Fourier transformation of the Green's function in the two-dimensional space of film plane, we obtain the following linear equations from which the spin wave energy spectrum can be solved:

$$[\omega I - P_k]G = F. \quad (7)$$

Here, we have defined vectors

$$\begin{aligned} G^{\mathrm{T}} &= (G_1^+, \cdots G_\mu^+, \cdots G_L^+) \\ F^{\mathrm{T}} &= [(S_1^+, \cdots S_\mu^+, \cdots S_L^+), B], \end{aligned}, \quad (8)$$

where the subscripts indicate MLs. Now we choose

$$B_j = (S_j^z)^n S_j^-. \quad (9)$$

Then we can calculate the magnetization $\langle S_\mu^z\rangle$ of each ML by using the Green's function. On account of the translation invariant in each ML, $\langle S_{\mu i}^z\rangle = \langle S_\mu^z\rangle$. But the magnetization is different from ML to ML, so subscript μ remains there. Choosing $n = 0, 1, 2 \ldots$, in Eq.(9), we can calculate the magnetization for the spin quantum number $S = 1/2,1,3/2, \ldots$. Therefore, this method enables us to calculate the magnetization of arbitrary S.

The method described above is only for calculating the z-direction magnetization. Recently a new technique has been developed to calculate magnetization with three components by use of the MBGFMn.[17,24–27] In this paper, we do not need to calculate all the three components of the magnetization. Therefore, the method described above is more than sufficient for the present purpose.

The total magnetization of AFM layer is zero when L_2 is even. For the whole system, we find that to define two kinds of magnetizations is useful in the discussion below. One is the total magnetization M_{t} of the FM layer, i.e.

$$M_{\mathrm{t}} = \sum_{\alpha=1}^{L_1}\langle S_\alpha^z\rangle. \quad (10)$$

M_{t} varies with the FM thickness and temperature. Obviously, the thicker the FM layer and the lower the temperature, the larger the value of M_{t}. The other is the averaged magnetization M, i.e.

$$M = \frac{M_{\mathrm{t}}}{L_1}. \quad (11)$$

We will see that M_{t} and M are closely related to H_{E} and H_{C}, respectively.

In this paper, the parameters in Hamiltonian expression (1) are set as follows: $S = 1$, $J_\alpha = 200\,\mathrm{T}$ and $K_\alpha = 1\,\mathrm{T}$, $\alpha = 1, 2, \ldots, L$; in the FM layer, $J_{\alpha,\alpha+1} = 100\,\mathrm{T}$, $\alpha = 1, 2, \ldots, L_1$; in the AFM layer, $J_{\alpha,\alpha+1} = -100\,\mathrm{T}$, $\alpha = L_1+1, L_1+2, \ldots, L$. The interfacial coupling strength are taken as $J_{\mathrm{F-AF}} = J_{L_1,L_1+1} = 1\,\mathrm{T}$ except those in Fig.12. The interfacial coupling is set to be two orders of magnitude less than J_α in FM and AFM layers. The magnetizations M and M_{t} are in units of spin, so that they are dimensionless quantities.

3. Numerical results and discussion

3.1. Transition temperature and magnetization

M_{t} and M as functions of FM thickness and temperature are calculated when the AFM thickness is fixed and the external field is absent. Figure 2 shows M vs T curves for different values of L_1 with $L_2 =$

6 MLs. M decreases with temperature rising. At a transition temperature, referred to hereafter as T_S, M becomes zero. In this system, the FM layer has a Curie point T_C and the AFM layer has a Néel point T_N. Both are called transition temperature. However, the transition point T_S is not simply equal to either T_C of FM layer or T_N of AFM layer. Figure 3 shows the T_S as a function of the FM thickness.

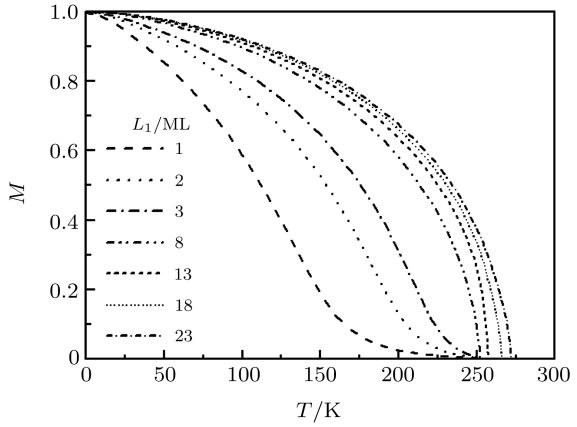


Fig.2. Averaged magnetization M as a function of T for different FM thicknesses.

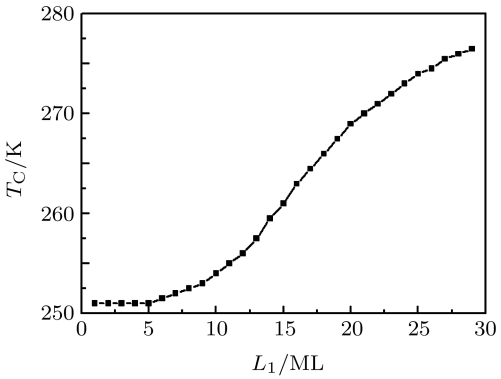


Fig.3. Transition point T_S as a function of L_1.

On the one hand, when the FM thickness becomes thicker, T_S increases, and the increase gradually becomes slower. On the other hand, when the FM thickness becomes thinner, T_S decreases, and the decrease becomes slower when L_1 is close to 1ML. When L_1 = 1 ML, T_S = 251 K. This is different from the case of pure FM film. For a pure FM film, T_C rises rapidly from the 1ML thickness and T_C rises more and more slowly with the FM thickness increasing,[24] which is in agreement with experimental results in Ref.[28]. It does not tend to a certain value as the thickness decreases to 1ML. The numerical results in this paper reflect the effect of the AFM layer. When L_1 is much larger than L_2, T_S is close to the Curie point T_C of the FM layer. On the contrary, when L_1 tends to 1ML, T_s is close to T_N of the AFM layer. This is because the interfacial coupling is assumed to be rather weak: it is two orders of magnitude less than the exchange coupling in FM and AFM layers.

The Curie point of a 1 ML FM film is about T_C = 150 K. The Néel point of a 6 ML AFM layer is T_N = 250 K. When the two layers couple to each other, the magnetization of the FM layer does not reach zero until T = 251 K (see dashed line in Fig.2 which shows a tail). The same analysis applies to the other curves such as L_1 = 2 MLs in Fig.2.

As already mentioned, the thicker the FM layer is, the larger the total magnetization M_t is. Figure 4 shows that M_t increases with L_1 linearly. As for the averaged magnetization M, it can be seen from Fig.2 that a thinner FM layer has a smaller M when the temperature is between zero and T_S. Figure 5 plots the M vs L_1 curves at different temperatures. At each temperature, as L_1 becomes large, M approaches a saturation value, which is the magnetization of the bulk material at this temperature.

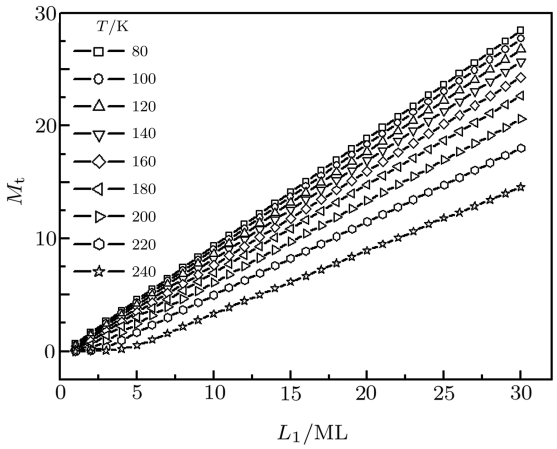


Fig.4. The total magnetization M_t versus the FM thickness L_1 at different temperatures.

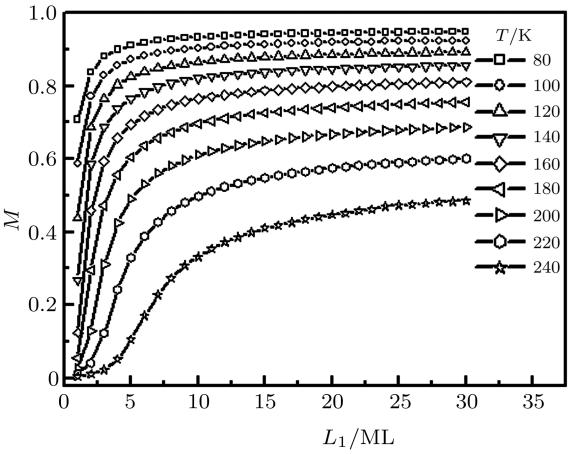


Fig.5. Averaged magnetization M versus the FM thickness L_1 at different temperatures.

3.2. Coercivity H_C and exchange bias H_E

The hysteresis loops are calculated when an external field is applied. Figure 6 shows the hysteresis loops for various FM thicknesses. The exchange bias H_E is determined by the separation between the centre of the hysteresis loop and $B = 0$. The half-width of the hysteresis loop is the coercivity H_C. As shown in Fig.6, H_E decreases with L_1, while H_C and the area of the loops increase with L_1. The reason is that M_t and M become smaller and more easily affected by the field when L_1 is smaller. Although the magnetizations of MLs are different from each other, all of them reverse uniformly. That is to say, all MLs of the FM layer have the same H_C and H_E.

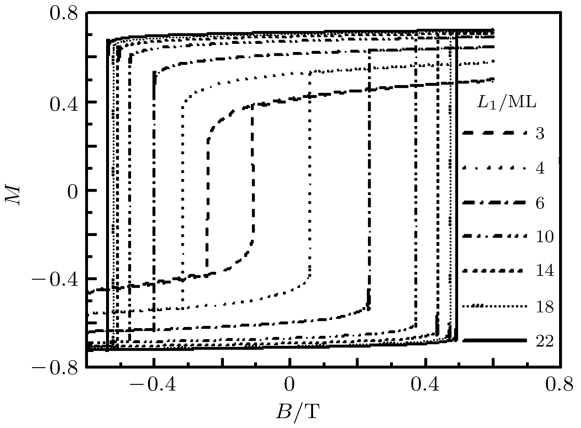


Fig.6. The hysteresis loops for different FM thicknesses at temperature 200K.

Figure 7 shows the hysteresis loops at various temperatures with $L_1 = 5$ MLs. As the temperature becomes higher, the areas of the loops, H_C and H_E become smaller. This is because higher temperatures result in smaller values of M_t and M, and the magnetizations are more easily affected by the magnetic field.

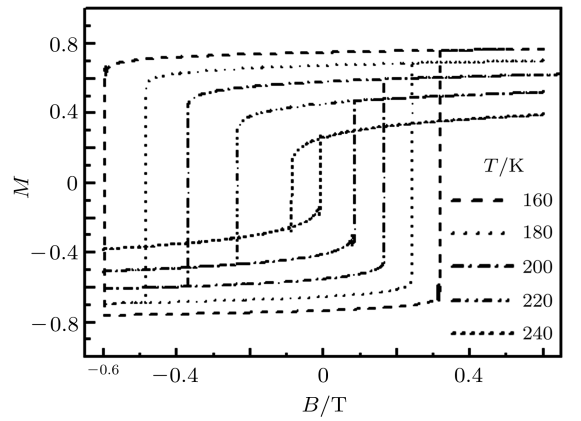


Fig.7. The hysteresis loops at various temperatures when L_1=5MLs.

In spite of our model being ideal, the calculated hysteresis loops are quite similar to those obtained from experiments (see, e.g., the hysteresis loop curves in Ref.[6]).

From the calculated hysteresis loops, we can evaluate exchange bias H_E and coercivity H_C. Figure 8 shows H_C versus L_1 at various temperatures. As the FM thickness increases, H_C increases rapidly and then tends to a saturation value. When M is smaller, the magnetic field needed to reverse the magnetic moment is smaller. So the thinner the FM layer is, the lower the H_C is. M tends to a saturation value when the FM layer is thick enough. Correspondingly, H_C also tends to a saturation value. The behaviours of approaching saturation values are the same for both Figs.5 and 8. Therefore, we think that H_C is closely related to the averaged magnetization M.

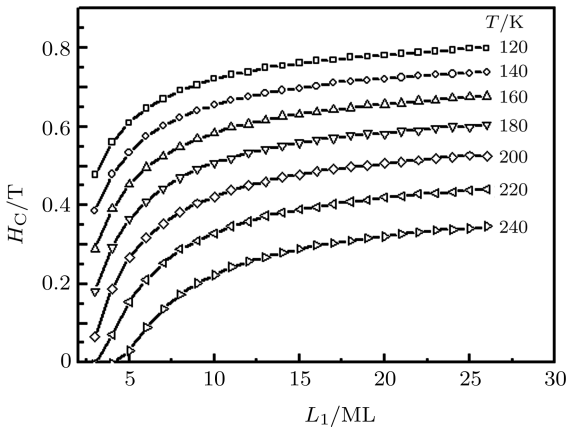


Fig.8. The coercivity H_C versus the FM thickness at various temperatures.

The exchange bias is induced by the AFM layer through the interfacial coupling. We regard this coupling as equivalent to the EBF exerted on the FM layer. Here we present an approximate expression of the EBF. In fact, Hamiltonian expression (1) can be written as $H = H_F + H_{AF} + H_I$, where H_F and H_{AF} are the Hamiltonians of FM and AFM layers, respectively. The interfacial coupling Hamiltonian between FM and AFM layers is as follows:

$$H_I = -J_{F-AF} \sum_i \boldsymbol{S}_{L_1 i} \cdot \boldsymbol{S}_{L_1+1 i}. \tag{12}$$

It can be approximately written as

$$H_I = -J_{F-AF} \sum_i S^z_{L_1 i} \langle S^z_{L_1+1 i} \rangle = -h_{ex} \sum_i S^z_{L_1 i}. \tag{13}$$

The quantity h_{ex} is equivalent to a field applied to interfacial FM ML, which is the so-called EBF. Both

the definition given here and that defined in Ref.[15] are proportional to $\langle S^z_{L_1+1}\rangle$, the magnetic moment of the interfacial AFM ML. However $\langle S^z_{L_1+1}\rangle$ in Ref.[15] is assumed always to be unchanged in direction and in magnitude so that it is simplified into a parameter in Hamiltonian. While in the present case, $\langle S^z_{L_1+1}\rangle$ is calculated from the statistical average of spin operator. Therefore, the magnitude of $\langle S^z_{L_1+1}\rangle$ varies with temperature. The effect of the EBF is mainly embodied in the calculated $H_{\rm E}$ shown in Figs.9–11.

Figure 9 shows $H_{\rm E}$ versus L_1 for various temperatures. With temperature rising and L_1 increasing, the exchange bias $H_{\rm E}$ descends. But as the FM layer is thick enough, $H_{\rm E}$ seems hard to decrease further and the curves become flat. We think that this manifests the EB as an interfacial effect. Roughly speaking, the acting effect of EBF may arrive at some depth, say, l, in the FM layer. When L_1 is smaller than l, the whole FM layer is affected. When L_1 is larger than l, only a part of the FM layer is affected, so that the effect of the EBF becomes weaker and $H_{\rm E}$ becomes flat. The depth l should vary with temperature. For example, it is seen from Fig.9 that at $T = 240\,{\rm K}$ the curve becomes flat at about 10 MLs. Similarly, the acting depth at a lower temperature, say, $T = 120\,{\rm K}$ is more than 15 MLs.

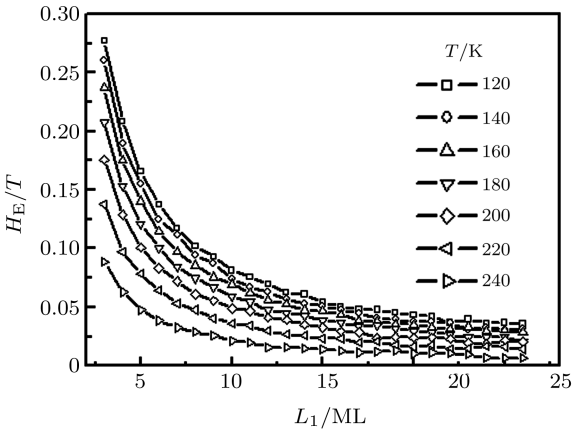


Fig.9. The exchange bias $H_{\rm E}$ versus the FM thickness at various temperatures.

Figure 10 shows that $H_{\rm E}$ is nearly linearly proportional to $1/L_1$ and decreases with temperature rising, which accords with the results of experiments.[2,16,29,30] In view of the total magnetization $M_{\rm t}$ being proportional to L_1, we deem that $H_{\rm E}$ is the inverse of $M_{\rm t}$. Figure 10 shows that the higher the temperature, the smaller the slope of line. The reason is that at smaller values of L_1, $H_{\rm E}$ decreases with temperature faster than at larger values of L_1 as can be seen in Fig.9. This feature is also indicated in Fig.11.

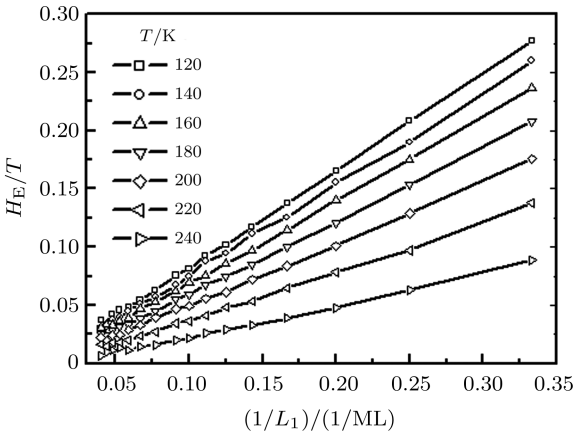


Fig.10. The dependence of $H_{\rm E}$on $1/L_1$ at various temperatures.

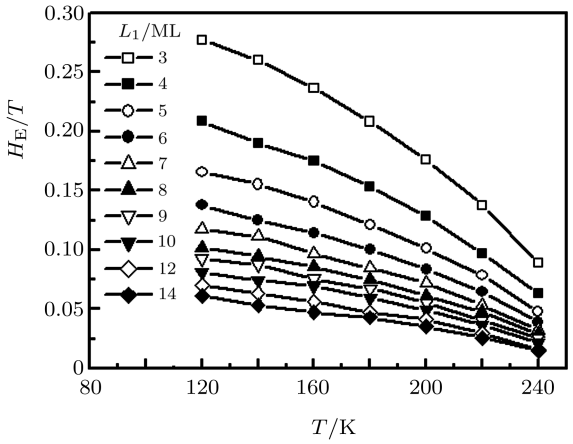


Fig.11. Temperature dependence of $H_{\rm E}$ for various film thicknesses.

Figure 11 shows the dependence of $H_{\rm E}$ on temperature for various values of L_1. These curves are similar to those in Fig.2 of Ref.[16] and Fig.4 of Ref.[30]. $H_{\rm E}$ decreases with temperature increasing when L_1 is fixed. The thicker the FM layer, the less the slope. For larger values of L_1 these curves become more compact.

The EBF $h_{\rm ex}$ defined in Eq.(13) consists of two factors: $\langle S^z_{L_1+1}\rangle$ and coupling parameter $J_{\rm F-AF}$. The discussion above concerns the effect of factor $\langle S^z_{L_1+1}\rangle$. Now we examine the effect of $J_{\rm F-AF}$. Figure 12 shows the $H_{\rm E}$ versus the $J_{\rm F-AF}$ with $L_1 = 5\,{\rm MLs}$ and $T = 200\,{\rm K}$. $H_{\rm E}$ increases with $J_{\rm F-AF}$ almost linearly.

Figure 12 also shows the $H_{\rm C}$ versus the $J_{\rm F-AF}$. The variation tendency of $H_{\rm C}$ is contrary to that of $H_{\rm E}$. This difference is also revealed in Figs.6 and 7. The analysis in Ref.[15] about this characteristic is

likely still to be applicable here. Note that when the variation of temperature is taken into account, it dose not hold true any more. The increasing of temperature leads to both $H_{\rm E}$ and $H_{\rm C}$ to drop as seen in Figs.8–11.

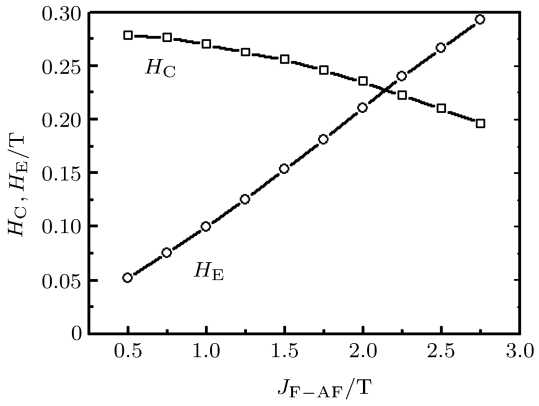


Fig.12. $H_{\rm C}$ and $H_{\rm E}$ versus the interfacial exchange coupling parameter $J_{\rm F-AF}$ with FM thickness L_1=5MLs and temperature $T = 200\,{\rm K}$.

Hereinbefore, the AFM thickness is fixed. Now we discuss the influences of the change of the AFM thickness on $H_{\rm C}$ and $H_{\rm E}$. The calculated $H_{\rm C}$ and $H_{\rm E}$ as functions of L_2 are plotted in Fig.13.

As L_2 is beyond a certain value, say, about 4-5 MLs in Fig.13, $H_{\rm E}$ is almost invariant with the AFM layer thickness. In our view, since the EB is primarily an interfacial effect, the variation of the AFM thickness does not change the configuration of interface such as the net magnetization of the AFM surface and the interfacial coupling strength. When L_2 is less than 4 MLs, $H_{\rm E}$ drops to zero. We ascribe this phenomenon to a pinning effect of AFM layer. The pinning effect means that the magnetic moments of the AFM surface ML are fixed in one direction, independent of the changing of FM magnetization, as long as the external field is not too high. That is the physical reason of EB. However, the pinning effect plays the role only when L_2 is above a certain value. When L_2 is too small, the magnetic moment in the interface of the AFM layer is easily affected by the magnetic moment of FM layer. This makes the orientation of $\langle S^z_{L_1+1}\rangle$ follow the change of the magnetization of the FM layer. In the present case, the interfacial coupling is FM exchange. The 'follow' here means that the magnetic moments of the (L_1+1)th ML are always parallel to those of FM layer. Thus, the EBF vanishes, and $H_{\rm E}$ becomes zero. The smallest thickness of an AFM layer which generates a nonzero $H_{\rm E}$ is called pinning thickness. From Fig.13, it seems that the pinning thickness is almost invariant with L_1 increasing.

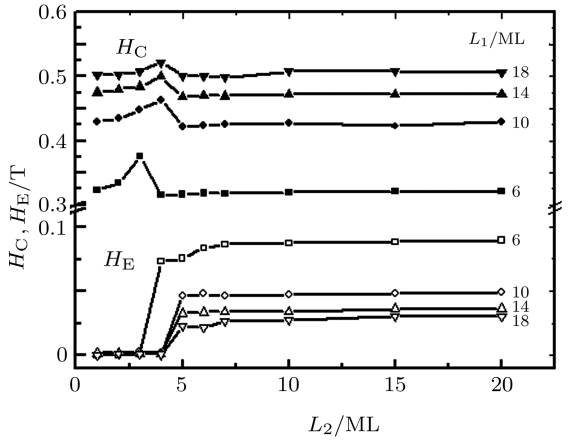


Fig.13. $H_{\rm E}$ (solid symbols) and $H_{\rm C}$ (open symbols) versus the AFM thickness L_2 with various FM thicknesses and temperature $T = 200\,{\rm K}$. The lines are for guiding eyes.

We compare $H_{\rm E}$ curves in Fig.13 with those in Fig.10 of Ref.[2] obtained experimentally. Qualitatively, they are quite similar to each other, but quantitatively, there exist two differences. One is that the pinning thickness in the experiment is much larger than that shown here in Fig.13. The other is that in the experiment, $H_{\rm C}$ decreases with L_2 when it is beyond the pinning thickness. However, different experiments give different results. Both $H_{\rm E}$ and $H_{\rm C}$ curves in Fig.13 are qualitatively the same as those in Fig.2 of Ref.[6]. We think that the films fabricated in experiments contained domains, impurities etc, which weaken the pinning ability of AFM layer, thus, lead to thicker pinning thicknesses. In some experiments a thicker film contains more grains, which makes $H_{\rm C}$ decrease.

Figure 13 shows two features of $H_{\rm C}$ curves. One is that, above the pinning thickness, $H_{\rm C}$ is almost invariant with L_2. This is still ascribed to the fact that the variation of AFM layer thickness does not change the interfacial configuration. The other is that when L_2 is just 1 ML less than the pinning thickness, $H_{\rm C}$ rises. The reason is as follows. Owing to the vanishing of the pinning, the magnetic moments of the (L_1+1)th ML keep the same orientation as that of the FM layer, and this is equivalent to adding one ML to the FM layer. $H_{\rm C}$ of an (L_1+1) ML FM layer is higher than that of an L_1 ML FM layer. As the film thickness further decreases, $H_{\rm C}$ decreases as can be seen in Fig.8.

4. Summary

In this paper, the exchange bias of the FM/AFM bilayer system in an uncompensated case is investigated by use of the MBGFM.

We first calculate the dependence of the magnetization on temperature and the thickness of the FM layer L_1, with no external magnetic field applied. When L_1 is much greater than L_2, the order-to-disorder transition temperature T_S of the bilayer tends to the Curie point T_C. When the thickness of the FM layer is close to zero, T_S tends to the T_N of the AFM layer. At each temperature, M_t is proportional to L_1 and M tends to a saturation value which is the magnetization of the bulk material.

Then an external field is applied to compute the hysteresis loops. At a fixed temperature, the thicker the FM layer, the larger the H_C and the smaller the H_E. When L_1 reaches a large value, H_C approaches a saturation value, a behaviour that is consistent with M. H_E is linearly proportional to the reciprocal of L_1. Therefore, it is concluded that H_E is inverse of M_t.

From our calculation, the EB is ascribed to the effect of an EBF. The EBF is approximately the product of the magnetization in the surface of the AFM layer and the interfacial coupling strength. Generally speaking, the larger the EBF, the stronger the EB is. The calculated results show that H_E is nearly linearly proportional to the interfacial coupling strength.

In most cases, the variations of H_E and H_C with parameter are contrary as long as the temperature is fixed. Both H_E and H_C decrease with temperature rising.

The influence of AFM layer thickness L_2 is also discussed. It reveals that there exists a pinning thickness of AFM layer, below which the EB disappears.

The calculated results in this paper are compared with experimental results where available. It seems that the dependence of H_E on either FM or AFM layer thickness is qualitatively in agreement with the experimental results. As for H_C, there are some differences from experimental results. We think that the coercivity is easily affected by the factors such as domains and polycrystals generated in the fabrication of FM materials. Our present model does not contain such kind of factors.

In this paper, we consider only the case that interfacial coupling is FM coupling. The case of interfacial AFM coupling can also be discussed, and the conclusions are the same except that the magnetizations of the L_1th and (L_1+1)th MLs always point to opposite directions.

References

[1] Meiklejohn W P and Bean C P 1956 *Phys. Rev.* **102** 1413
[2] Nogues J and Schuller I K *J. Magn. Magn. Mater.* 1999 **192** 203
[3] Jin S, Tiefil T H, Gyorgy E M, Chen L H, Waszczak J V and Kammlott G W 1992 *IEEE Trans. Magn.* **28** 3192
[4] Dimitrov D V, Murthy A S, Hadjipanayis G C and Swann C P 1996 *J. Appl. Phys.* **79** 5106
[5] He K 2006 *Chin. Phys.* **15** 449
[6] Zhai Z H, Teng J, Li B H, Wang L J, Yu G H and Zhu F W 2006 *Acta Phys. Sin.* **55** 2064 (in Chinese)
[7] Malozemoff A P 1987 *Phys. Rev.* B **35** 3679
[8] Koon M C 1997 *Phys. Rev. Lett.* **78** 4865
[9] Suhl H and Schuller Ivan K 1998 *Phys. Rev.* B **58** 258
[10] Keller J, Miltenyi P, Beschoten B, Guntherodt G, Nowak U and Usadel K D 2002 *Phys. Rev.* B **66** 014431
[11] Kiwi M 2001 *J. Magn. Magn. Mater.* **234** 584
[12] Thuy N P, Tuan N A, Phuoc N N, Nam N T, Hien T D and Hai N H 2006 *J. Magn. Magn. Mater.* **304** 41
[13] Schulthess T C and Butler W H 1998 *Phys. Rev. Lett.* **81** 4516
[14] Yang F Y and Chien C L 2000 *Phys. Rev. Lett.* **85** 2597
[15] Wang H Y and Dai Z H 2004 *Commun. Theor. Phys.* **42** 141
[16] Takano K, Kodama R H, Berkowitz A E, Cao W and Thomas G 1997 *Phys. Rev. Lett.* **79** 1130
[17] Fröbrich P, Jensen P J and Kuntz P J 2000 *Eur. Phys. J.* B **13** 477
[18] Moschel A and Usadel K D 1994 *Phys. Rev.* B **49** 1268
[19] Bogolyubov N N and Tyablikov S V 1959 *Sov. Phys. Dokl.* **4** 589
[20] Wang H Y, Zhou Y S, Wang C Y and Lin D L 2002 *Chin. Phys.* **11** 167
[21] Anderson F B and Callen H B 1964 *Phys. Rev.* **136** A1068
[22] Lines M E 1967 *Phys. Rev.* **156** 534
[23] Schwieger S, Kienert J and Nolting W 2005 *Phys. Rev.* B **71** 024428
[24] Wang H Y, Jen S U and Yu J Z 2006 *Phys. Rev.* B **73** 094414
[25] Henelius P, Fröbrich P, Kuntz P J, Timm C and Jensen P J 2002 *Phys. Rev.* B **66** 094407
[26] Fröbrich P, Jensen P J, Kuntz P J and Ecker A 2000 *Eur. Phys. J.* B **18** 579
[27] Pini M G, Politi P and Stamps R L 2005 *Phys. Rev.* B **73** 014454
[28] Feng Q, Huang Z G and Du Y W 2003 *Acta Phys. Sin.* **52** 2906 (in Chinese)
[29] Leighton F, Fitzsimmons M R, Hoffmann A, Dura J, Majkrzak C F, Lund M S and Schuller I K 2002 *Phys. Rev.* B **65** 064403
[30] Smardz L 2002 *J. Magn. Magn. Mater.* **240** 273